A Density Functional Theory Study of the Interactions of H_2O with H−ZSM-5, Cu−ZSM-5, and Co−ZSM-5

Mark J. Rice, Arup K. Chakraborty,* and Alexis T. Bell

Materials Sciences Division, Lawrence Berkeley National Laboratory and Departments of Chemistry and Chemical Engineering, University of California, Berkeley, California 94720-1462

Received: February 11, 1998

The interactions of water with H−ZSM-5, Cu−ZSM-5, and Co−ZSM-5 have been investigated by density functional theory (DFT). Calculations were also performed to determine the thermodynamics of metal removal from the zeolite. For all three forms of ZSM-5, water adsorbs by direct interaction of the O atom with the cation and hydrogen bonding of one of the two H atoms with an oxygen atom in the zeolite framework. The magnitude of the energy of adsorption of one H_2O molecule decreases in the order Cu−ZSM-5 (Cu as Cu^+) > Co−ZSM-5 (Co as $Co^{2+}(OH^-)$) > H−ZSM-5 > Cu−ZSM-5 (Cu as $Cu^{2+}(OH^-)$). Adsorption of a second H_2O molecule occurs with a smaller binding energy, which decreases in the order Cu−ZSM-5 (Cu as Cu^+) > Cu−ZSM-5 (Cu as $Cu^{2+}(OH^-)$) > Co−ZSM-5 (Co as $Co^{2+}(OH^-)$) > H−ZSM-5. At 800 K, demetalation to form a gaseous metal hydroxide species is unfavorable thermodynamically but will occur spontaneously if the final product is a metal oxide. Demetalation of Cu is projected to occur much more readily than demetalation of Co, in good agreement with experimental observation.

Introduction

Copper and cobalt cations exchanged into ZSM-5 zeolites have been investigated extensively as catalysts for the decomposition and reduction of NO.[1−19] While only Cu−ZSM-5 is active for NO decomposition to N_2 and O_2, both Cu−ZSM-5 and Co−ZSM-5 are active for NO reduction by hydrocarbons. Co−ZSM-5 is more active than Cu−ZSM-5 for NO reduction by methane, but the reverse is true for NO reduction by propane.[17] To be effective as catalysts for the selective catalytic reduction of NO emissions from either lean-burning engines or stationary sources, such as power plants, metal cation-exchanged zeolites must be hydrothermally stable. Experimental studies show that Cu−ZSM-5 loses a substantial part of its activity both reversibly and irreversibly in the presence of steam, whereas the loss in activity of Co−ZSM-5 upon exposure to steam is largely reversible.[8,12,13] Reversible loss of activity is attributed to the competitive adsorption of H_2O by the metal cation, whereas irreversible loss in activity is attributed to the removal of metal cations from cation-exchange sites in the zeolites. The latter process can be accompanied by the formation of small particles of metal oxide either within the pores of the zeolite or on the exterior of the zeolite crystals.[20,21] In view of these observations, there is considerable interest in understanding the fundamental factors affecting the hydrothermal stability of transition-metal cation-exchanged ZSM-5.

Recent studies have shown that the physical and chemical properties of metal cations substituted into ZSM-5 can be investigated effectively by means of quantum density functional theory (DFT) calculations.[22−25] DFT studies of the local bonding of Cu cations exchanged into ZSM-5 have also been reported, as well as an analysis of the thermochemistry of NO decomposition over Cu−ZSM-5.[22−24,26] In the present study, DFT calculations have been used to compare the local geometries of Cu−ZSM-5 and Co−ZSM-5 and to investigate the strength of H_2O adsorption on these catalysts. Additional calculations have been performed to determine the thermodynamics of removing Cu and Co cations from cation-exchange positions and forming either metal hydroxide or oxide species.

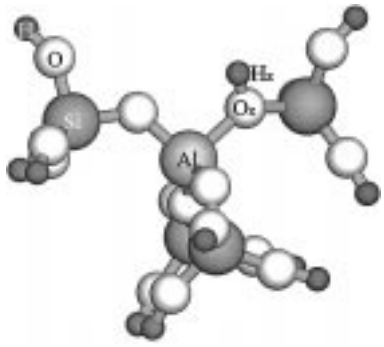

Figure 1. Structure of H^+Z^-.

Theoretical Methods

The zeolite was represented by a cluster containing 34 atoms, five of which are T atoms (Si or Al) (see Figure 1). The Al atom is placed in the T12 site, and the O atoms at the edge of the cluster are fixed in the crystallographic positions of these atoms in ZSM-5.[27] These terminal O atoms are bond to H atoms located 1.0 Å from each of the O atoms and oriented in the direction of what would normally be the next Si atom. During the calculation, all of the atoms in the cluster including the charge-compensating cation (e.g., H^+, Cu^+, $(CuOH)^+$, $(CoOH)^+$), excluding the OH groups terminating the cluster, are allowed to relax geometrically. A smaller cluster containing seven atoms was used for frequency calculations to minimize the computational cost. This cluster consists of an $[H_2Al(OH)_2]^-$ anion. All of the atoms in this cluster are relaxed during the course of DFT calculations. Charge compensation by a metal cation is treated in the same manner as the larger cluster.

Gradient-corrected density functional theory calculations were carried out using the B3LYP hybrid method to represent the

S1089-5639(98)01108-6 CCC: $15.00
Published on Web 09/02/1998

TABLE 1: Metal−Oxide Diatomics

molecule	method	r_e (Å)	ω (cm^{-1})	D_0 (eV)
CoO	DFT/B3LYP	1.59	906	4.25
	CCSD(T)[a]	1.62	909	3.64
	experiment	1.63[b]	853[c]	3.94 ± 0.14[d]
CuO	DFT/B3LYP	1.76	623	2.59
	CCSD(T)[a]	1.77	572	2.66
	experiment	1.72[g]	640[e]	2.85 ± 0.15[f]

[a] Reference 31. [b] Reference 43. [c] Reference 44. [d] Reference 45. [e] Reference 46. [f] Reference 47.

TABLE 2: Water Dimer (H_2O-H_2O) (kcal/mol)

method	basis set	ΔE
experiment[a]		−5.4 ± 0.7
DFT/B3LYP	6-31G**	−7.54
	6-31G**(++)[b]	−5.43
	6-31G**++	−5.40
	6-311G**++	−5.14

[a] Reference 32. [b] Diffuse functions only added to the hydrogen-bonded oxygen and hydrogen.

effects of electron exchange and correlation. The 6-31G basis set was used to describe all but the transition-metal atoms. For transition-metal atoms, the effective core potentials and associated valence basis functions of Hay and Wadt were used.[28−30] Polarization functions were added to all atoms except the transition-metal atom and the cluster-terminating OH groups of the large cluster.

The adequacy of the DFT method and basis sets was tested by comparing the calculated properties of CuO(g) and CoO(g) with those measured experimentally and those reported for high-level quantum calculations. Table 1 shows that DFT with the B3LYP functional and the basis sets described above yield values of the equilibrium bond distance and vibrational frequency that are in good agreement with both experiment and the results of coupled cluster calculations involving singles and doubles and estimates of triples (CCSD(T)).[31] This is a particularly stringent test because the degree of correlation changes greatly from the bonded to the dissociated state. The dissociation energy determined from DFT/B3LYP calculations is acceptable relative to experiment and high-level theoretical estimates of the dissociation energy of the M−O bond.

To test the validity of our methods for handling hydrogen bonding, we calculated the energy of forming a water dimer. The results of these calculations are presented in Table 2 and compared with experiment. The equilibrium geometry of the dimer was identified using a 6-31G** basis set, after which the dimer binding energy was recalculated using a basis set enhanced with diffuse functions for either the hydrogen bonding O and H atoms or all of the atoms. Table 2 shows that the addition of diffuse functions to only those atoms involved in hydrogen bonding yields an estimate of the dimer binding energy in good agreement with experiment and with the results of calculations conducted with much larger basis sets.[32] On the basis of these results, it was decided that adequate accuracy could be achieved by carrying out single-point calculations of the interactions of H_2O with H−ZSM-5, Co−ZSM-5, and Co−ZSM-5 with diffuse functions added to only those atoms involved in hydrogen bonding, starting with a converged cluster geometry obtained from calculations not involving diffuse functions.

Thermodynamic values were calculated using standard statistical mechanical methods.[33] For gaseous species, the translational, rotational, vibational, and electronic partition functions were calculated. Because the zeolite cluster is a model for a solid, the translational and rotational partition functions were assumed not to contribute. An analogous smaller, fully relaxed cluster was used to estimate the vibrational partition function, since this avoids the technical problems associated with the size and constrained nature of the larger cluster. While this approach to calculating vibrational frequencies is not perfect, the final thermodynamic values are relatively resistant to small errors in individual frequencies. For example, an error of 50 cm^{-1} in the lowest vibration mode of water at 500 K yields errors of only 0.06 and 0.07 kcal/mol in the internal energy and free energy, respectively. Since there is generally low occupation of excited electronic states, we assumed that only ground-state degeneracy contributed to the electronic partition functions.

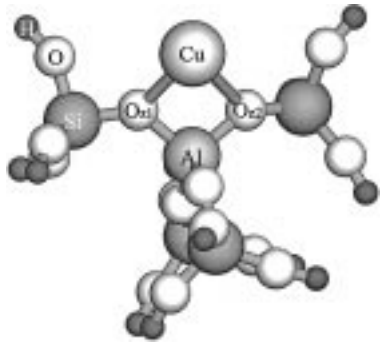

Figure 2. Structure of Cu^+Z^-.

Results

Local Structure of H−ZSM-5, Cu−ZSM-5, and CoZSM-5. The structures of the clusters used to represent H−ZSM-5, Cu−ZSM-5, and Co−ZSM-5 are presented in Figures 1−3. In the case of Cu−ZSM-5, structures are shown in which the copper cation is either Cu^+ (Figure 2) or $Cu^{2+}(OH)^-$ (see Figure 3). For purposes of convenience, we will refer to the clusters appearing in Figures 1−3 and elsewhere as H^+Z^-, Cu^+Z^-, $Cu^{2+}(OH)^-Z^-$, and $Co^{2+}(OH)^-Z^-$.

The equilibrium values of the H_z-O_z bond distance and the O_{z1}-Al−O_{z2} bond angle for the cluster representing H^+Z^- are 0.970 Å and 96.0°, respectively. These values are consistent with those reported in previous DFT studies, 0.970−0.984 Å and 91.1−102.1°.[34−38]

Figure 2 shows the structure of Cu^+Z^-. The Cu−O_{z1}, Cu−O_{z2}, and Cu−Al bond distances are 1.95, 2.06, and 2.64 Å, respectively. These values are greater than those reported previously by Trout et al.[22] based on DFT/LSDA calculations using an uncontracted Huzinaga basis set. In that study, the Cu−O_{z1}, Cu−O_{z2}, and Cu−Al bond distances were 1.9, 2.0, and 2.4 Å, respectively. These small differences can be attributed to the overbinding usually predicted by the LSDA approximation. Comparison can also be made with unrestricted HF calculations reported by Blint[39] in which 6-31G** basis functions were used for O and H and ECP's and associated valence basis functions were used for Si, Al, and Cu. Calculations were carried out for a 2T, unconstrained cluster terminated by OH groups. The two Cu−O_z distances obtained in that work are equal to 2.14 Å.

The structures of $Cu^{2+}(OH)^-Z^-$ and $Co^{2+}(OH)^-Z^-$ are illustrated in Figure 3. The Cu−O_{z1}, Cu−O_{z2}, and Cu−(OH) bond distances for $Cu^{2+}(OH)^-Z^-$ are 1.92, 2.05, and 1.77 Å and the Co−O_{z1}, Co−O_{z2}, and Co−(OH) bond distances for $Co^{2+}(OH)^-Z^-$ are 1.99, 2.06, and 1.78 Å. For comparison, Blint[39] obtained a value of 2.03 Å for the two Cu−O_z bond lengths using the methods described above. The Cu−O_{z1}, Cu−

Figure 3. Structure of $Cu^{2+}(OH)^{-}Z^{-}$ and $Cu^{2+}(OH)^{-}Z^{-}$.

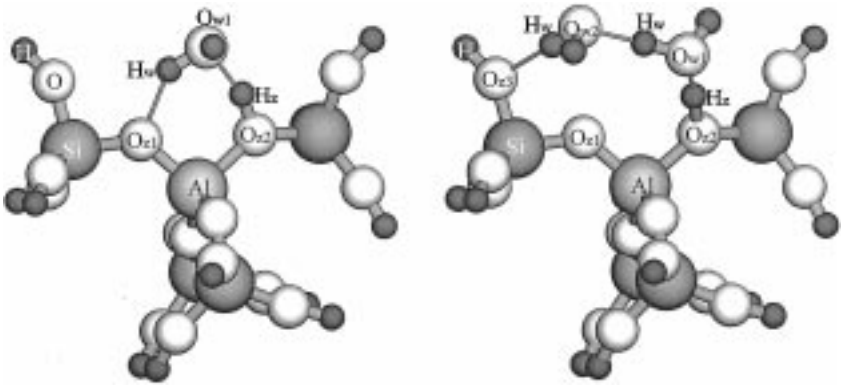

Figure 4. Structure of one and two waters bound to $H^{+}Z^{-}$.

TABLE 3: Selected Bond Distances (Å) and Bond Angles (deg) for H_2O on $H^{+}Z^{-}$

cluster size	method	no. of waters	$r(O_{z2}H_z)$	$O_{z1}AlO_{z2}$	$r(O_{z1}O_{w1})$	$r(O_{w1}H_z)$	$r(O_zH_w)$	$r(O_{w1}H_w)$	$r(O_{w2}H_w)$	$r(O_{w1}O_{w2})$	ref
5T	DFT/B3LYP	1	1.05	97.2	2.49	1.46	1.75	0.99			this work
5T	DFT/B3LYP	2	1.15	98.7	2.41	1.26	1.72	1.02	0.99	2.57	this work
5T	DFT/BP	1	1.05	104.2	2.52	1.51	1.71	1.01			35
5T	DFT/BP	2	1.11	98.8	2.46	1.37	1.92	1.00		2.70	35
3T	MP2	1	1.02	97.2		1.61	1.81	0.99			40
3T	DFT/BLYP	1	1.03			1.61	1.77	1.01			34
							1.81				
4T	DFT/BLYP	2	1.06			1.50	1.79	1.01	1.00		34

O_{z2}, and Cu−(OH) bond distances for $Cu^{2+}(OH)^{-}Z^{-}$ reported by Trout et al.[22] are 2.0, 2.1, and 1.7 Å, respectively.

Local Structure of H_2O Adsorbed on H−ZSM-5, Cu−ZSM-5, and CoZSM-5. The structure of H−ZSM-5 with one and two H_2O molecules bound is shown in Figure 4, and selected bond distances and angles are reported in Table 3. Also shown in Table 3 for comparison are the results of similar calculations reported in the literature. Taking into consideration the differences in cluster size, calculational approach, and basis sets, the results of the present calculations for the interaction of one H_2O molecule with H−ZSM-5 lead to geometries in good agreement with those reported previously.[34,35,40] Interaction of the Brønsted-acid proton with the O atom of H_2O leads to slight elongation of the H_z-O_z bond distance but does not result in proton transfer. Hydrogen bonding by one of the H atoms of H_2O with the zeolite framework is observed and the H_w-O_{z1} bond distance for this H atom is 1.75 Å.

The structure of two H_2O molecules interacting with H−ZSM-5 presented in Figure 4 differs from that reported previously.[34] In the present study, the second H_2O molecule is hydrogen bonded to the first molecule as well as to the zeolite. While this arrangement contributes to a lengthening of the H_z-O_z bond to 1.15 Å, proton transfer to form $H_3O^{+}\cdots H_2O$ does not occur. This finding is consistent with that of Gale[34] but differs from that of Krosnner and Sauer;[35] however, it is noted that the location of the second H_2O molecule relative to the first differs in both of these studies, as well as differing relative to that shown in Figure 5. These differences are also apparent upon inspection of Table 3. It is noteworthy that the heat of adsorption for the second molecule calculated in this study and those reported by Gale[34] and by Krossner and Sauer[35] lie within a few kilocalories of each other. These similar energies for several different geometries of two H_2O adsorbed on H−ZSM-5 may reflect the presence of multiple minima of comparable depth on the potential surface. Here too, differences in cluster size, method of cluster termination, the presence or absence of structural constraints, and the details of the quantum calculations may contribute to the observed differences in geometry.

Figures 5−7 show the structures of one and two H_2O molecules interacting with Cu−ZSM-5 and Co−ZSM-5. In each case, the first H_2O molecule is bound through its O atom to the metal cation and is further stabilized by hydrogen bonding.

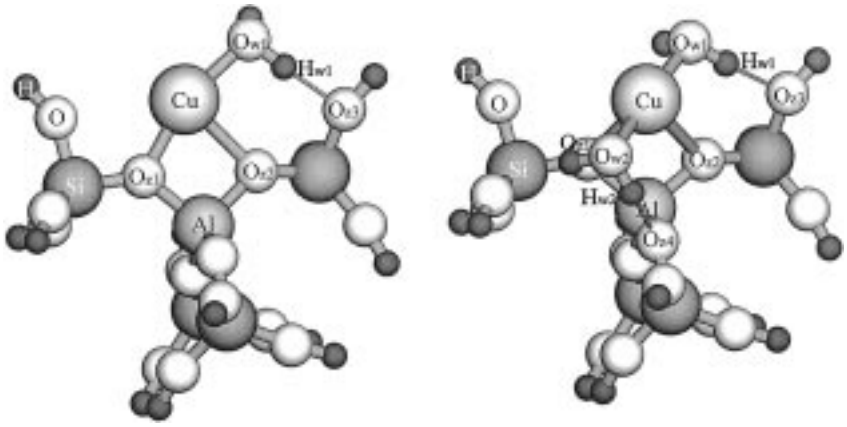

Figure 5. Structure of one and two waters bound to Cu^+Z^-.

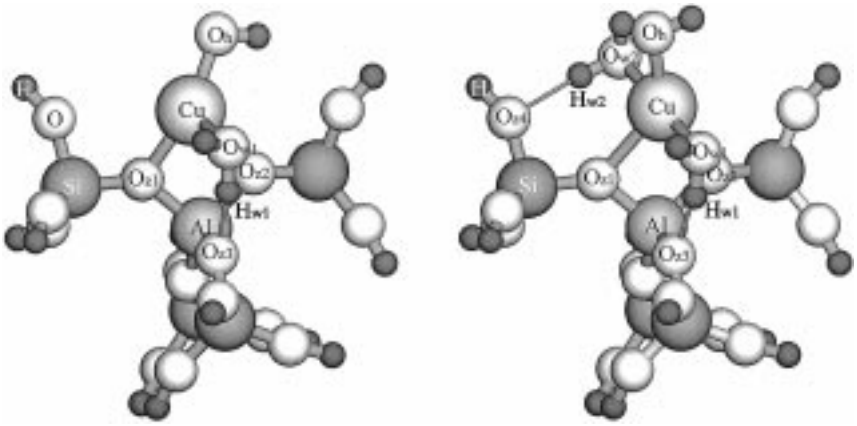

Figure 6. Structure of one and two waters bound to $Cu^{2+}(OH)^-Z^-$.

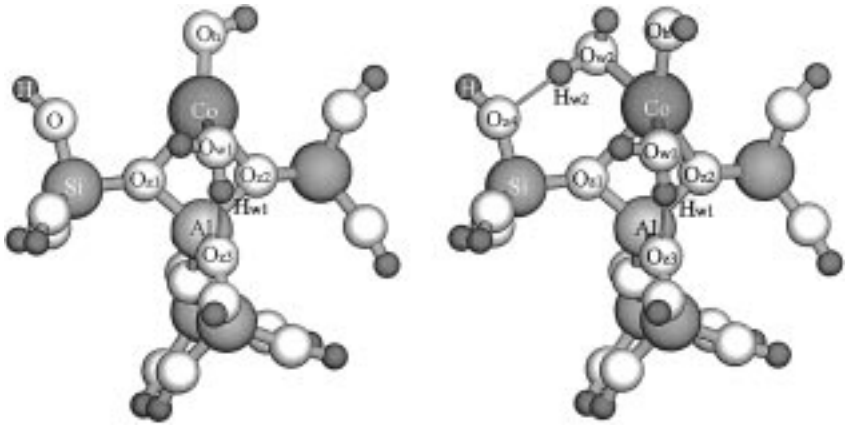

Figure 7. Structure of one and two waters bound to $Co^{2+}(OH)^-Z^-$.

A similar type of bonding occurs for the second H_2O molecule. Selected bond distances for these two structures are presented in Table 4 and compared with those for Cu^+Z^-, $Cu^{2+}(OH)^-Z^-$, and $Co^{2+}(OH)^-Z^-$. Of significance are the increases in the Cu−O_{z1} and Cu−O_{z2} bond lengths as first one and then two molecules of H_2O are adsorbed. A similar trend has been reported earlier by Blint.[39] A similar trend is observed for $Cu^{2+}(OH)^-Z^-$ and $Co^{2+}(OH)^-Z^-$ in Figures 6 and 7, respectively, but the bond lengthening is less pronounced.

Thermodynamics of H_2O Adsorption. The energies for the adsorption of H_2O on H−ZSM-5 are presented in Table 5. Also listed for comparison are the adsorption energies from previously reported quantum calculations[34,35,40] and from experimental measurement.[41] Good agreement is observed between the present results and those of Krausner and Sauer,[35] which were based on both MP2 and DFT calculations conducted with a 5T cluster to represent the Brønsted-acid site in faujasite. The present results also agree closely with those obtained by Zygmunt et al.[40] and Gale[34] on the basis of DFT calculations carried out with either a 3T or a 4T cluster, respectively. The degree of consistency between different investigators is all the more reassuring given that there are significant differences in the calculational approach used by each group (i.e., cluster size, method of cluster termination, whether the cluster is constrained, the method of handling electron exchange and correlation, and the basis set used). The calculated values of ΔE and those estimated from the experimental values of $\Delta H°(298\ K)$ are significantly different for the case of one adsorbed H_2O molecule but not for the adsorption of a second H_2O molecule. Since

TABLE 4: Selected Bond Distances (Å) for H_2O on Cu−ZSM-5 and Co−ZSM-5

cluster	no. of waters	r (MO_{z1})	r(MO_{z2})	r(MO_h)	r(MO_{w1})	r(MO_{w2})	r($H_{w1}O_{z3}$)	r($H_{w2}O_{z4}$)
Cu^+Z^-	0	1.95	2.06					
Cu^+Z^-	1	1.96	2.31		1.98		1.69	
Cu^+Z^-	2	2.42	2.79		1.98	2.00	1.73	1.88
$Cu^{2+}(OH)^-Z^-$	0	2.05	1.92	1.77				
$Cu^{2+}(OH)^-Z^-$	1	2.34	1.98	1.78	1.92		1.69	
$Cu^{2+}(OH)^-Z^-$	2	2.42	2.23	1.89	2.03	2.06	1.63	2.01
$Co^{2+}(OH)^-Z^-$	0	2.06	1.99	1.78				
$Co^{2+}(OH)^-Z^-$	1	2.12	2.10	1.81	2.11		1.73	
$Co^{2+}(OH)^-Z^-$	2	2.30	2.07	1.87	2.17	2.16	1.70	1.82

TABLE 5: Comparison of Calculated Heats of H_2O Adsorption on H−ZSM-5 with Previously Published Theoretical and Experimental Results

method	cluster size	cluster termination	cluster constraints	no. of waters	basis set	ΔE (kcal/mol)	ref
DFT/B3LYP	5T	OH	Edge	1	6-31G(**)	−19.7	this work
DFT/B3LYP	5T	OH	Edge	2	6-31G(**)	−11.8	this work
MP2	5T	H	None	1	DZP(H,S,Al);TZP(O)	−18.9	35
DFT/BP	5T	H	None	1	DZP(H,S,Al);TZP(O)	−17.9	35
DFT/BP	5T	H	None	2	DZP(H,S,Al);TZP(O)	−14.2	35
MP2	3T	OH	None	1	6-31G(++)	−22.1	40
DFT/BLYP	3T	OH	None	2	DZVP2	−16.0	34
DFT/BLYP	4T	OH	None	1	DZVP2	−12.3	34
experiment				1		−12.1	41
experiment				2		−8.1	41

TABLE 6: Water Adsorption Energy (kcal/mol)

reaction	ΔE	$\Delta H°$(500 K)	$\Delta G°$(500 K)	$\Delta G°$(800 K)
$H_2O + Cu^+Z^- \rightarrow (H_2O)Cu^+Z^-$	−29.09	−27.29	−10.25	−0.21
$H_2O + Cu^{2+}(OH)^-Z^- \rightarrow (H_2O)Cu^{2+}(OH)^-Z^-$	−17.80	−15.76	+0.98	+10.82
$H_2O + Co^{2+}(OH)^- \rightarrow (H_2O)Co^{2+}(OH)^-Z^-$	−26.19	−23.90	−7.54	+2.04
$H_2O + (H_2O)Cu^+Z^- \rightarrow (H_2O)_2Cu^+Z^-$	−19.78	−19.26	−4.12	+4.78
$H_2O + (H_2O)Cu^{2+}(OH)^-Z^- \rightarrow (H_2O)_2Cu^{2+}(OH)^-Z^-$	−13.85	N. A.	N. A.	N. A.
$H_2O + (H_2O)Co^{2+}(OH)^-Z^- \rightarrow (H_2O)_2Co^{2+}(OH)^-Z^-$	−13.53	N. A.	N. A.	N. A.

the uncertainties in the experimental values of ΔE are not known, it is difficult to comment further.

Values of ΔE, $\Delta H°$(500 K), and $\Delta G°$(500 K) for the adsorption of one and two molecules of H_2O on Cu^+Z^-, $Cu^{2+}(OH)^-Z^-$, and $Co^{2+}(OH)^-Z^-$ are presented in Table 6. The values of ΔE and $\Delta H°$(500 K) for the adsorption of one H_2O molecule decrease in the order $Cu^{2+}(OH)^-Z > Co^{2+}(OH)^-Z > Cu^+Z^-$. For the adsorption of a second H_2O molecule, the values of ΔE decrease in the order $Cu^{2+}(OH)^-Z^- \approx Co^{2+}(OH)^-Z > Cu^+Z^-$ and in all cases the magnitude of ΔE is smaller than that for the adsorption of the first molecule of H_2O. Table 6 demonstrates, as well, that while $\Delta H°$(500 K) is negative in all instances, the value of $\Delta G°$(500 K) can be either positive or negative. This result is a direct consequence of the negative entropy change associated with the adsorption of H_2O. Thus, the adsorption of one H_2O molecule at 500 K is seen to be favorable for Cu^+Z^- and $Co^{2+}(OH)^-Z^-$ but marginally unfavorable for $Cu^{2+}(OH)^-Z^-$. At 800 K, the temperature at which NO reduction by hydrocarbons typically reaches a maximum, the value of $\Delta G°$ is positive or very close to zero.

The binding energies calculated for the interactions of H_2O with Cu^+Z^- and $Cu^{2+}(OH)^-Z^-$ can be compared with similar calculations reported by Blint.[39] In that study, unrestricted Hartee−Fock calculations were carried out using a 3T model to represent the zeolite. During the calculations, the geometry of the adsorbed H_2O molecules was allowed to relax but not the geometry of the cluster representing the zeolite. A combination basis set was used. The bridging O atoms were described by the D95v** basis of Dunning and Hay,[42] the Cu, Si, and Al atoms were described by the effective core potential and accompanying valence basis set of Wadt and Hay,[28−30] and the remaining H and O atoms are described by the 3-21G basis set. Blint reports adsorption energies of −28.2 and −23.6 kcal/mol for adsorption of the first and second water molecules on Cu^+Z^-, respectively, and adsorption energies of −21.3 and −30.7 kcal/mol for the adsorption of the first and second water molecules on $Cu^{2+}(OH)^-Z^-$. The adsorption energies for H_2O on $Cu^{2+}(OH)^-Z^-$ are significantly larger in magnitude than those found in the present study. By contrast, while the binding energy for one H_2O molecule interacting with Cu^+Z^- is close to that reported here, the binding energy for the adsorption of the second H_2O molecule is significantly larger in magnitude. The discrepancies between Blint's work and ours can be attributed to a variety of causes, including the use of a small, rigid cluster, neglecting of the effects of electron correlation, and small basis sets for describing the atoms in H_2O.

Hydrothermal Stability of Cu−ZSM-5 and Co−ZSM-5. Table 7 list values of ΔE, $\Delta H°$(800 K), and $\Delta G°$(800 K) for the reactions $M^{2+}(OH)^-Z^- H^+Z^- + [MO](g)$ and $M^{m+}(OH)^-_{(m-1)}Z^- + nH_2O(g) \rightarrow H^+Z^- + [M(OH)_m(H_2O)_{n-1}](g)$ ($m = 1, 2$ and $n = 1, 2, 3$) at 800 K. $\Delta H°$(800 K) and $\Delta G°$(800 K) for the first of these reactions are positive and relatively large in magnitude, suggesting that the reaction does not occur to any significant degree. When H_2O is present, the value of $\Delta H°$(800 K) decreases monotonically as n increases from 1 to 3, due to the stabilization of the metal hydroxide by hydration. However, the increasingly negative entropy of reaction offsets this benefit. As a consequence, $\Delta G°$(800 K) is positive in all cases and increases in magnitude for n greater than 0, with the exception of Cu^+Z^-. In this case, $\Delta G°$(800 K) passes through a minimum when $n = 2$. The net result of these calculations is that even in the presence of steam at 800 K, it is unlikely that

TABLE 7: Metal Extraction To Form Mobile Metal Hydroxide (kcal/mol)

$$M^{m+}(OH)^{-}_{(m-1)}Z^{-} + aH_2O(g) \rightarrow H^{+}Z^{-} + M(OH)_m(H_2O)_{(a-1)}(g)$$

reaction	ΔE	$\Delta H°$(800 K)	$\Delta G°$(800 K)
$Cu^{2+}(OH)^{-}Z^{-} \rightarrow H^{+}Z^{-} + CuO(g)$	+81.50	+80.06	+37.50
$Co^{2+}(OH)^{-}Z^{-} \rightarrow H^{+}Z^{-} + CoO(g)$	+108.36	+107.07	+64.98
$Cu^{+}Z^{-} + H_2O(g) \rightarrow H^{+}Z^{-} + Cu(OH)(g)$	+29.31	+29.29	+19.47
$Cu^{2+}(OH)^{-}Z^{-} + H_2O(g) \rightarrow H^{+}Z^{-} + Cu(OH)_2(g)$	+24.09	+24.01	+16.62
$Co^{2+}(OH)^{-}Z^{-} + H_2O(g) \rightarrow H^{+}Z^{-} + Co(OH)_2(g)$	+32.63	+32.49	+25.72
$Cu^{+}Z^{-} + 2H_2O(g) \rightarrow H^{+}Z^{-} + Cu(OH)(H_2O)(g)$	−0.64	+2.73	+14.79
$Cu^{2+}(OH)^{-}Z^{-} + 2H_2O(g) \rightarrow H^{+}Z^{-} + Cu(OH)_2(H_2O)(g)$	+9.20	+11.97	+26.50
$Co^{2+}(OH)^{-}Z^{-} + 2H_2O(g) \rightarrow H^{+}Z^{-} + Co(OH)_2(H_2O)(g)$	+8.57	+11.72	+26.48
$Cu^{+}Z^{-} + 3H_2O(g) \rightarrow H^{+}Z^{-} + Cu(OH)(H_2O)_2(g)$	−18.33	−10.72	+31.93
$Cu^{2+}(OH)^{-}Z^{-} + 3H_2O(g) \rightarrow H^{+}Z^{-} + Cu(OH)_2(H_2O)_2(g)$	−7.94	−2.30	+36.18
$Co^{2+}(OH)^{-}Z^{-} + 3H_2O(g) \rightarrow H^{+}Z^{-} + Co(OH)_2(H_2O)_2(g)$	−8.59	−2.38	+36.64

TABLE 8: Metal Extraction To Form Metal Oxide Solid (kcal/mol)

$$M^{m+}(OH)^{-}_{(m-1)}Z^{-} + aH_2O(g) + ({}^{b}/_{2})O_2(g) \rightarrow H^{+}Z^{-} + [MO_{(a+b+m-1)}](s)$$

reaction	$\Delta H°$(298 K)
$Cu^{+}Z^{-} + {}^{1}/_{2}H_2O(g) \rightarrow H^{+}Z^{-} + {}^{1}/_{2}Cu_2O(s)$	−43.3
$Cu^{+}Z^{-} + {}^{1}/_{2}H_2O(g) + {}^{1}/_{4}O_2(g) \rightarrow H^{+}Z^{-} + CuO(s)$	−60.8
$Cu^{2+}(OH)^{-}Z^{-} \rightarrow H^{+}Z^{-} + {}^{1}/_{2}Cu_2O(s) + {}^{1}/_{4}O_2(g)$	−18.3
$Cu^{2+}(OH)^{-}Z^{-} \rightarrow H^{+}Z^{-} + CuO(s)$	−35.7
$Co^{2+}(OH)^{-}Z^{-} \rightarrow H^{+}Z^{-} + CoO(s)$	−10.2
$Co^{2+}(OH)^{-}Z^{-} + {}^{1}/_{6}O_2(g) \rightarrow H^{+}Z^{-} + {}^{1}/_{3}Co_3O_4(s)$	−24.4

a substantial amount of either Cu or Co will be lost from the zeolite as a consequence of forming hydrated or nonhydrated CuOH(g), $Cu(OH)_2$(g), or $Co(OH)_2$(g). However, it is still conceivable that these species could participate in the redistribution of Cu or Co within the zeolite or serve as intermediates for the formation of small particles of copper or cobalt oxide.

A quite different picture emerges if we consider the reaction $M^{m+}(OH)^{-}_{(m-1)}Z^{-} + aH_2O(g) + ({}^{b}/_{2})O_2(g) \rightarrow H^{+}Z^{-} + [MO_{(a+b+m-1)}](s)$ ($m = 1, 2$). Table 8 shows that in this case $\Delta H°$(298 K) is moderately negative in all cases due in large measure to the Madelung stabilization energy associated with the formation of the bulk oxide phase. This stabilization is readily apparent when the values of $\Delta H°$(298 K) given in Table 7 for $M^{2+}(OH)^{-}Z^{-} \rightarrow H^{+}Z^{-} + [MO](g)$ are compared with the values of $\Delta H°$(800 K) given in Table 8 for $M^{2+}(OH)^{-}Z^{-} \rightarrow H^{+}Z^{-} + [MO](s)$. Since the effect of temperature on the value of $\Delta H°$ is small, it can be neglected. In all of the cases listed in Table 8, the enthalpy of reaction for the release of Cu from the zeolite is significantly more favorable than that for the release of Co. These findings are in good agreement with experimental observation[8,12,13] and explain the greater hydrothermal stability of Co−ZSM-5 relative to Cu−ZSM-5.

Conclusions

In recent years, hybrid density functional theory has advanced to near chemical accuracy. Nevertheless, energetic chemical accuracy (±1 kcal/mol) has not yet been achieved. In systems where the chemical character changes dramatically, as for the dissociation energies of metal oxide diatomics (see Table 1), errors can be large. On the other hand, if systems have similar chemical character and if the energetic differences are larger than the estimated errors, hybrid density functional theory can reveal qualitative trends. In this paper, we have carried out calculations that provide insight into the interactions of water with H−ZSM-5, Cu−ZSM-5, and Co−ZSM-5. Our major findings are summarized below.

H−ZSM-5 adsorbs water solely through the formation of hydrogen bonds. When only one H_2O molecule is involved, the O atom of H_2O hydrogen bonds to the proton of the Brønsted-acid site in the zeolite and one of the two H atoms of H_2O forms a hydrogen bond with an O atom in the zeolite framework. Introduction of a second H_2O molecule results in the formation of one hydrogen bond between an H atom of the first H_2O molecule and the O atom of the second H_2O molecule and the formation of a second hydrogen bond between one of the H atoms of the second H_2O molecule and an O atom in the zeolite framework. No evidence of proton transfer is observed when either one or two molecules of H_2O are adsorbed on H−ZSM-5.

The adsorption of H_2O on ZSM-5-exchanged Cu^{+}, $Cu^{2+}(OH)^{-}$, or $Co^{2+}(OH)^{-}$ occurs via the formation of a bond between the O atom of H_2O and the metal cation and a hydrogen bond formed between one of the two H atoms of H_2O and an O atom in the zeolite framework. When a second molecule of H_2O adsorbs, the mode of bonding is identical to that for the first molecule of H_2O. In all cases, the adsorption of water lengthens the bonds between the metal cation and the O atoms in the zeolite framework to which the metal is bonded. The extent of M−O bond lengthening increases with the number of H_2O molecules adsorbed, indicating a weakening of the attachment of the metal cation to the zeolite framework. The Gibbs free energy of adsorption of a single molecule of H_2O decreases in magnitude in the order: $Cu^{+}Z^{-} > Co^{2+}(OH)^{-}Z^{-} > Cu^{2+}(OH)^{-}Z^{-}$. The Gibbs free energy change for the adsorption of a second H_2O molecule is less than that for the first and decreases in magnitude in the order: $Cu^{+}Z > Cu^{2+}(OH)^{-}Z^{-} > Co^{2+}(OH)^{-}Z^{-}$.

Demetalation via the reactions $M^{2+}(OH)^{-}Z^{-} \rightarrow H^{+}Z^{-} + [MO](g)$ and $M^{m+}(OH)^{-}_{m-1}Z^{-} + nH_2O(g) \rightarrow H^{+}Z^{-} + [M(OH)m(H_2O)_{n-1}](g)$ ($m = 1, 2$ and $n = 1, 2, 3$) is thermodynamically unfavorable, but these processes may contribute to the migration of metal cations within the zeolite. By contrast, demetalation via the reaction $M^{m+}(OH)^{-}_{(m-1)}Z^{-} + aH_2O(g) + ({}^{b}/_{2})O_2(g) \rightarrow H^{+}Z^{-} + [MO_{(a+b+m-1)}](s)$ ($m = 1, 2$) is thermodynamically favorable due to the Madelung stabilization energy associated with the formation of the bulk oxide phase. The driving force for demetalation of $Cu^{+}Z^{-}$ and $Cu^{2+}(OH)^{-}Z^{-}$ is significantly greater than that for $Co^{2+}(OH)^{-}Z^{-}$, which may help explain the greater stability of Co−ZSM-5 than Cu−ZSM-5 to demetalation observed experimentally during the selective catalytic reduction of NO by hydrocarbons in the presence of steam.

Acknowledgment. This work was supported by the Office of Industrial Technology of the U.S. Department of Energy under Contract DE-AC03-SF7600098. Computational resources

were provided by the National Energy Research Supercomputer Center and the San Diego Supercomputer Center.

References and Notes

(1) Iwamoto, M.; Yoke, S.; Sakai, K.; Kagawa, S. *J. Chem. Soc., Faraday Trans.* **1981**, *77*, 1629.

(2) Iwamoto, M.; Furukawa, H.; Kagawa, S. *New Developments in Zeolite Science and Technology*; Murukama, Y., Ichijima, A., Ward, J. W., Eds.; Elsevier: Amsterdam, 1986; p 943.

(3) Iwamoto, M.; Hamada, H. *Catal. Today* **1991**, *10*, 57.

(4) Iwamoto, M.; Yahiro, H.; Tanada, K.; Mozino, Y.; Mine, Y.; Kagawa, S. *J. Phys. Chem.* **1991**, *95*, 3727.

(5) Li, Y.; Armor, J. N. *Appl. Catal. B* **1992**, *1*, L31.

(6) Teraoka, Y.; Ogawa, H.; Furukawa, H.; Kagawa, S. *Catal. Lett.* **1992**, *12*, 361.

(7) Li, Y.; Battavio, P. J.; Armor, J. N. *J. Catal.* **1993**, *142*, 561.

(8) Li, Y.; Armor, J. N. *Appl. Catal. B* **1993**, *2*, 239.

(9) Kharas, K. C. C. *Appl. Catal. B* **1993**, *2*, 207.

(10) Zhang, Y.; Flytzani-Stephanopoulos, M. Catalytic Decomposition of Nitric Oxide over Promoted Copper-Ion-Exchanged ZSM-5 Zeolites. In *Environmental Catalysis*; Armor, J. N., Ed.; ACS Symposium Series 552; American Chemical Society: Washington, DC, 1994; p 7.

(11) Centi, G.; Nigro, C.; Perathoner, S.; Stella, G. Reactivity of Cu-Based Zeolites and Oxides in the Conversion of NO in the Presence or Absence of O_2. In *Environmental Catalysis*; Armor, J. N., Ed.; ACS Symposium Series 552; American Chemical Society: Washington, DC, 1994; p 22.

(12) Armor, J. N.; Farris, T. S. *Appl. Catal. B* **1994**, *4*, L11.

(13) Armor, J. N. *Catal. Today* **1995**, *26*, 147.

(14) Aylor, A. W.; Larsen, S. C.; Reimer, J. A.; Bell, A. T. *J. Catal.* **1995**, *157*, 592.

(15) Shelef, M. *Chem. Rev.* **1995**, *95*, 209.

(16) Campa, M. C.; De Rossi, S.; Ferraris, G.; Indovina, V. *Appl. Catal. B* **1996**, *8*, 315.

(17) Adelman, B. J.; Beutel, T.; Lei, G.-D.; Sachtler, W. M. H. *J. Catal.* **1996**, *158*, 327.

(18) Aylor, A. W.; Lobree, L. J.; Reimer, J. A.; Bell, A. T. An infrared study of NO reduction by CH_4 over Co−ZSM-5. In *Studies in Surface Science and Catalysis*; Hightower, J. W., Delgass, W. N., Iglesia, E., Bell, A. T., Eds.; Elsevier Science B. V.: New York, 1996; Vol. 101, p 661.

(19) Lobree, L. J.; Aylor, A. W.; Reimer, J. A.; Bell, A. T. *J. Catal.* **1997**, *169*, 188.

(20) Kharas, K. C. C.; Robota, H. J.; Datye, A. Deactivation of Cu−ZSM-5. In *Environmental Catalysis*; Armor, J. N., Ed.; ACS Symposium Series 552; American Chemical Society: Washington, DC, 1994; p 39.

(21) Jong, S.-J.; Cheng, S. *Appl. Catal. A* **1995**, *126*, 51.

(22) Trout, B. L.; Chakraborty, A. K.; Bell, A. T. *J. Phys. Chem.* **1996**, *100*, 4173.

(23) Trout, B. L.; Chakraborty, A. K.; Bell, A. T. *J. Phys. Chem.* **1996**, *100*, 17582.

(24) Hass, K. C.; Schneider, W. F.; Ramprasad, R.; Adams, J. B. *J. Phys. Chem. B* **1996**, *101*, 4353.

(25) Blint, R. J. *J. Phys. Chem.* **1996**, *100*, 257.

(26) Yokomichi, Y.; Yamabe, T.; Ohtsuka, H.; Kakumoto, T. *J. Phys. Chem.* **1996**, *100*, 14424.

(27) Olson, D. H.; Kokotallo, G. T.; Lawton, S. L.; Meier, W. M. *J. Phys. Chem.* **1981**, *85*, 2238.

(28) Hay, P. J.; Wadt, W. R. *J. Chem. Phys.* **1985**, *82*, 270.

(29) Wadt, W. R.; Hay, P. J. *J. Chem. Phys.* **1985**, *82*, 284.

(30) Hay, P. J.; Wadt, W. R. *J. Chem. Phys.* **1985**, *82*, 299.

(31) Bauschlicher, C. W., Jr.; Maitre, P. *Theor. Chim. Acta* **1995**, *90*, 189.

(32) Novoa, J. J.; Sosa C. *J. Phys. Chem.* **1995**, *99*, 15837.

(33) McQuarrie, D. A. *Statistical Mechanics*; HarperCollins Publisher Inc.: New York, 1973.

(34) Gale, J. D. *Top. Catal.* **1996**, *3*, 169.

(35) Krossner, M.; Sauer, J. *J. Phys. Chem.* **1996**, *100*, 6199.

(36) Greatbanks, S. P.; Hillier, I. H.; Burton, N. A.; Sherwood, P. *J. Chem. Phys.* **1996**, *105*, 3770.

(37) Brand, H. V.; Redondo, A.; Hay, P. J. *J. Mol. Catal. A* **1997**, *121*, 45.

(38) Gonzales, N. O.; Bell, A. T.; Chakraborty, A. K. *J. Phys. Chem. B* **1997**, *101*, 10058.

(39) Blint, R. J. *J. Phys. Chem.* **1996**, *100*, 19518.

(40) Zygmunt, S. A.; Curtiss, L. A.; Iton, L. E.; Erhardt, M. K. *J. Phys. Chem.* **1996**, *100*, 6663.

(41) Ison, A.; Gorte, R. J. *J. Catal.* **1984**, *89*, 150.

(42) Dunning, T. H.; Hay, P. J. Gaussian basis-sets for molecular calculation. In *Modern Theoretical Chemistry*; Schaeffer, H. R., Ed.; Plenum: New York, 1977; Vol. 3, p 1.

(43) Ram, R. S.; Jarman, C. N.; Bernath, P. F. *J. Mol. Spectrosc.* **1993**, *160*, 574.

(44) Green, D. W.; Reedy, G. T.; Kay, J. G. *J. Mol. Spectrosc.* **1979**, *78*, 257.

(45) Merer, A. J. *Annu. Rev. Phys. Chem.* **1989**, *40*, 407.

(46) Huber, K. P.; Herzberg, G. *Molecular Spectra and Molecular Structure. IV. Constants of Diatomic Molecules*; Van Nostrand Reinhold Ltd.: New York, 1979.

(47) Clemmer, D. E.; Dalleska, N. F.; Armentrout, P. B. *J. Chem. Phys.* **1991**, *95*, 5577.